

Hyperfine structure and lifetime measurements of the second-excited D states of rubidium and cesium by cascade fluorescence spectroscopy*

C. Tai,[†] W. Happer, and R. Gupta

Columbia Radiation Laboratory, Department of Physics, Columbia University, New York, New York 10027

(Received 7 April 1975)

The hyperfine structure of the second-excited D states of ^{87}Rb , ^{85}Rb , and ^{133}Cs has been measured by the method of cascade-radio-frequency spectroscopy and cascade-level crossing. The sign of the magnetic-dipole coupling constant A is determined by the method of cascade-decoupling and cascade-radio-frequency spectroscopy with narrow-band excitation. Lifetimes τ of some of these states are measured by the cascade-Hanle effect. We find that for ^{87}Rb , $A(5^2D_{3/2}) = 14.43 \pm 0.23$ MHz, $A(5^2D_{5/2}) = -7.44 \pm 0.10$ MHz, $\tau(5^2D_{3/2}) = 205 \pm 40$ nsec; for ^{85}Rb , $A(5^2D_{3/2}) = 4.18 \pm 0.20$ MHz, $A(5^2D_{5/2}) = -2.12 \pm 0.20$ MHz; for ^{133}Cs , $A(6^2D_{3/2}) = 16.30 \pm 0.15$ MHz, $A(6^2D_{5/2}) = -3.6 \pm 1.0$ MHz, $\tau(6^2D_{3/2}) = 57 \pm 15$ nsec.

I. INTRODUCTION

The fine-structure intervals of the D and F states of alkali-metal atoms are known to be anomalously small, and they are often inverted in all of the alkali-metal atoms except lithium.¹ To the lowest order, the hyperfine-structure intervals should be closely related to the fine-structure intervals, and it would be very interesting to measure the hyperfine structures of some non- P excited states with anomalous fine-structure intervals. When we began this work several years ago we could find only two reported measurements of D -state hyperfine structure. Archambault *et al.*² obtained $A < 0.33$ MHz for the $5^2D_{5/2}$ state of sodium and $0.195 < A < 0.45$ MHz for the $9^2D_{5/2}$ state of cesium. Brix and Kopfermann³ made a rough measurement of hyperfine constant A of the $6D_{3/2}$ state of Cs and they quote a value of $+0.0003 \text{ cm}^{-1}$. This deviates from the precise measurement reported in this work by 70%.

A major obstacle to experimental studies of the D states of alkali-metal atoms is the fact that they cannot be produced by direct optical excitation of the ground state. In the work reported in this paper we have populated D states by cascade transitions from higher-lying, optically excited P states. Our methods of measuring the D -state hyperfine structures, cascade-decoupling spectroscopy,^{4,5} cascade-radio-frequency spectroscopy,^{6,7} and cascade-level-crossing spectroscopy are all free of Doppler broadening and they have a precision which is ultimately limited only by the natural lifetime of the state.

II. THEORY

The basic scheme of our experiments is illustrated in Fig. 1. Polarized resonance light is used to excite atoms from the ground state g to an ex-

cited state e . In our experiments the excited state is the third excited P state of rubidium or cesium. The state e decays spontaneously to the branch state b , and some of the polarization imparted to the atom by the exciting light is carried over to the branch state. We do not observe the infrared fluorescence which is emitted when the atom decays from e to b . In our experiments the branch state b is the second excited D state of rubidium or cesium. We observe the fluorescent light emitted when the branch state b decays spontaneously to the final state f , which is the lowest P state of rubidium or cesium in our experiments. The fluorescence is observed as a function of the magnitude of an external static magnetic field. Radio-frequency (rf) magnetic fields are used to induce transitions between branch-state sublevels in some of our work.

In any given state, the coupling between the electronic angular momentum J , the nuclear spin I , and the external static magnetic field H is assumed to be adequately described by a Hamiltonian of the form

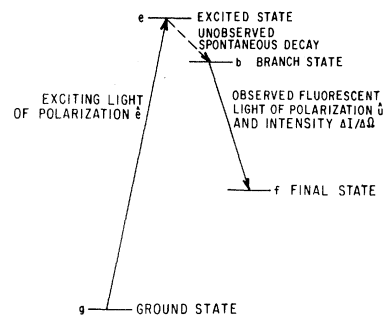


FIG. 1. Atomic states involved in a cascade-fluorescence experiment.

$$\mathcal{K}_0 = hA\vec{I} \cdot \vec{J} + hB \left(\frac{3(\vec{I} \cdot \vec{J})^2 + \frac{3}{2}\vec{I} \cdot \vec{J} - I(I+1)J(J+1)}{2I(2I-1)J(2J-1)} \right) + g_J \mu_B H J_z. \quad (1)$$

One aim of our work is to deduce the magnitudes of the coupling constants A and B from an analysis of the experimental data. We shall assume that the electronic g factors are given to sufficient accuracy by the Landé formula ($g_s \approx 2.00232$)

$$g_J = 1 + (g_s - 1) \frac{J(J+1) + S(S+1) - L(L+1)}{2J(J+1)}. \quad (2)$$

For white-light excitation by light of polarization \hat{e} and in the absence of any (rf) fields, it has been shown⁵ that the intensity ΔI of fluorescent light of polarization \hat{u} emitted into a small solid angle $\Delta\Omega$ is

$$\frac{\Delta I}{\Delta\Omega} = \sum_{\substack{m \\ jk \\ \mu\nu}} C_{mn;\mu} \langle j|\vec{p}|m\rangle \cdot \langle n|\vec{p}|k\rangle \langle k|\hat{u} \cdot \vec{p}|f\nu\rangle \times \langle f\nu|\hat{u}^* \cdot \vec{p}|j\rangle \langle m|\hat{e} \cdot \vec{p}|g\mu\rangle \langle g\mu|\hat{e}^* \cdot \vec{p}|n\rangle \times (\Gamma_e + i\omega_{mn})^{-1} (\Gamma_b + i\omega_{jk})^{-1}. \quad (3)$$

Here m and n label pairs of excited-state sublevels, j and k label pairs of branch-state sublevels, μ labels ground-state sublevels, and ν labels final-state sublevels. The momentum operator of the atom is \vec{p} . Frequency (energy $\times \hbar^{-1}$) differences are denoted by ω , and Γ_e and Γ_b denote the natural decay rates of the excited and branch states. All hfs (hyperfine-structure) energies are supposed to be defined by Hamiltonians of the form (1). Further discussion of (3) can be found in Ref. 5.

For white-light excitation by light of energy density u (erg cm⁻³ hz⁻¹) the factor C of (3) is independent of the subscripts m, n , and μ and is

$$C_{mn;\mu} = uK, \quad (4)$$

where the constant K is

$$K = \frac{4}{3} \left(\frac{e}{mc} \right)^2 \frac{\omega_{eb} \omega_{bf}}{\hbar^4 (\omega_{ge})^2} \frac{1}{(2J_g + 1)(2I + 1)}. \quad (5)$$

Occasionally it is necessary to take into account nonwhite optical excitation. If we represent the emission profile of the lamp by a series of Doppler-broadened lines of central frequencies ν_i and of collision broadened widths γ_i , then

$$C_{mn;\mu} = \sum_i U_i K \frac{\lambda}{2\pi i} \left(\frac{M_I M_V}{2R(T_I M_V + T_V M_I)} \right)^{1/2} \times [Z(\xi_{m\mu i}) - Z^*(\xi_{m\mu i})], \quad (6)$$

where $Z(\xi)$ is the plasma dispersion function,⁸

$$Z(\xi) = \frac{1}{\pi^{1/2}} \int_{-\infty}^{\infty} \frac{e^{-u^2}}{u - \xi} du, \quad (7)$$

with the argument

$$\xi_{m\mu i} = \frac{2\pi}{\lambda} \left(\frac{M_I M_V}{2R(M_V T_I + M_I T_V)} \right)^{1/2} \times [(1/\hbar)(E_m - E_\mu - h\nu_i) + i(\Gamma_v + \gamma_i + \gamma_v)]. \quad (8)$$

The gas constant is denoted by R . Also, λ is the mean wavelength of the exciting light, M_I and M_V are the atomic weights of the atoms in the lamp and in the vapor, respectively, T_I and T_V are the effective temperatures of atoms in lamp and in the vapor, γ_i and γ_v are collision broadening rates for the optical lines in the lamp and in the vapor, and E_m and E_μ denote energies (including the optical excitation energy) of the excited-state sublevel m and the ground-state sublevel μ . The natural decay rates of the atoms in the lamp and the atoms in the vapor are Γ_I and Γ_V , respectively ($\Gamma_V = \Gamma_e$ in our case). The total intensity (erg cm⁻³) of the lamp line l is U_l .

Equation (3) describes the fluorescent light intensity if no rf fields are present. However, in some of our work we use rf fields to induce transitions between excited-state sublevels. Then a sharp change of the fluorescent intensity is observed when the quasistatic external magnetic field tunes the energy splittings of the atoms into resonance with the radio frequency. Under the conditions of our work, the static field is large enough to ensure that the energy eigenstates of the excited P - and D -state atoms are very nearly uncoupled states. Then m_J and m_I , the azimuthal electronic and nuclear angular momenta, are very nearly good quantum numbers. Under those conditions, a rf resonance will be observed for each value of m_I for a rf transition between states m_J and $m_J - 1$ at a frequency given by

$$\nu = g_J (\mu_B/h) H + A m_I + \frac{hA^2}{2g_J \mu_B H} [(I^2 + I - m_I^2) + m_I(2m_J - 1)] + \dots + \frac{3B}{4} \frac{[I(I+1) - 3m_I^2](1 - 2m_J)}{J(2J-1)I(2I-1)} + \dots \quad (9)$$

In most of our experiments the magnetic field is sufficiently large and the quadrupole coupling constant B is sufficiently small that all transitions corresponding to a given value of m_I in (9) are driven at once and no trace of a dependence on m_J remains. If the excited state polarization is not too complicated, we will then observe an average frequency [the average of (9) for $m_J = J, J-1, \dots, -J+1$]

$$\nu(m_I) = g_J(\mu_B/h)H + Am_I + \frac{\hbar A^2}{2g_J\mu_B H} (I^2 + I - m_I^2). \quad (10)$$

The resonance line shape is a linear combination of a Bloch line shape and a Brossel-Bitter line shape, as discussed by Gupta *et al.*⁷ Since both line shapes are symmetric and of similar form for low rf powers, we do not attempt to make a careful study of the resonance line shapes when we analyze our experimental data, and we simply assume that the measured values of H and ν at the center of an rf resonance are related to each other by Eq. (10).

III. METHOD

A. Decoupling

In a decoupling experiment^{4,5} the atoms are excited by polarized resonance light and polarized fluorescent light is observed. The polarization of the fluorescent light is found to be a function of the external magnetic field and by analyzing the variation in polarization as a function of the magnetic field one can deduce the hyperfine structure of the excited states. Such decoupling experiments rely on changes in the longitudinal atomic polarization, in contrast to Hanle-effect⁹ or level-crossing¹⁰ experiments, which rely on changes in the transverse atomic polarization. Although the decoupling method is not very precise, it has the advantage that it is sensitive to the signs of the hyperfine coupling constants.

The apparatus we used to measure the polarization of the fluorescent radiation as a function of the magnetic field is shown schematically in Fig. 2. Resonance light from a microwave-powered lamp after a selection for frequency and circular

polarization, excites atoms in a Pyrex cell containing Rb or Cs to a P state. The D state that we are investigating is populated by spontaneous decay of P states. The intensity of this D -state fluorescence radiation is modulated by a rotating quarter-wave plate together with a fixed linear analyzer. The modulated light is detected by a photomultiplier tube, whose output is fed to a lock-in amplifier for synchronous detection. The alkali vapor cell is at the center of a pair of Helmholtz coils. By sweeping the magnetic field, we can observe the decoupling curve. The operating temperatures of the cells were about 125 °C for the $5D$ state of rubidium and 115 °C for the $6D$ state of cesium.

The polarized fluorescence intensity and the total fluorescence intensity are recorded simultaneously on a dual-channel strip-chart recorder or in the memory of a PDP8/S computer. The integration time is from 1 to 10 min at each magnetic field. The fluorescence polarization, i.e., the ratio of the polarized fluorescence to the total fluorescence, is our raw data.

We fit the curve of fluorescence polarization versus magnetic field by Eq. (3) by varying A , a_j , and b to minimize

$$\sum_i \left(P(H_i) - \sum_j a_j Y_j(H_i, A) - b \right)^2,$$

where $P(H_i)$ is our experimental result, H is the magnetic field, $Y_j(H_i, A)$ is the calculated polarization for cascades through different channels such as through $P_{1/2}$ or $P_{3/2}$ states, the a_j 's are parameters corresponding to the relative intensity of the fluorescence through different channels, and b represents an overall background level. Equation (3) is so complicated that the theoretical

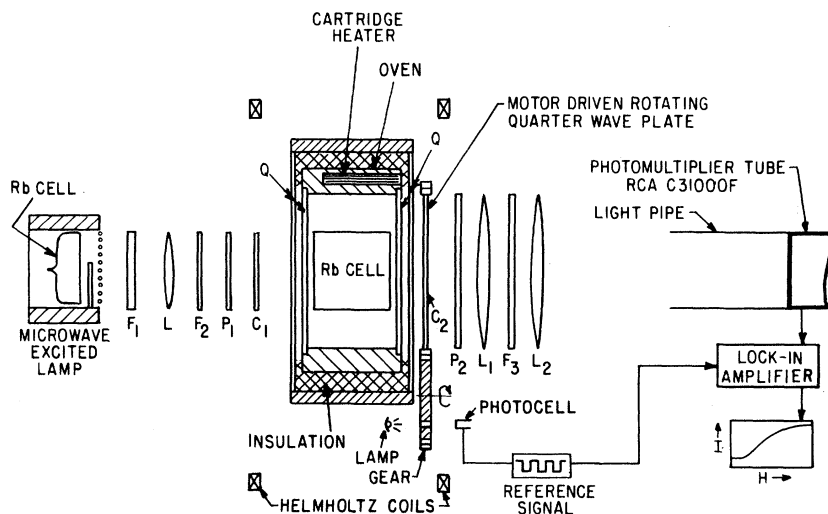


FIG. 2. Experimental arrangement for a cascade-decoupling experiment. F_1 and F_3 are interference filters; F_2 is a color glass filter; P_1 and P_2 are linear polarizers; C_1 and C_2 are quarter-wave plates; L , L_1 , and L_2 are lenses; and Q stands for quartz plates.

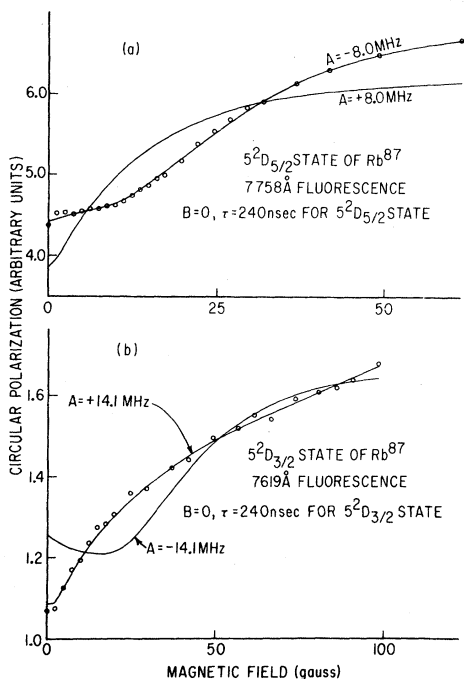


FIG. 3. Cascade-decoupling data for the $5D$ states of ^{87}Rb . The solid lines are calculated from the hyperfine parameters and lifetimes indicated in Table III. The points are experimental data. These data determine the signs and the approximate magnitudes of the D -state A values.

values of $Y_j(H_i, A) = (\Delta I / \Delta \Omega)(H_i, A)$ had to be evaluated numerically with an electronic computer program.

In fitting the experimental decoupling curves we usually used theoretical curves for $B=0$. We also investigated the influence of nonzero values of B on our fits and we found that the accuracy of our data was insufficient to distinguish between $B=0$

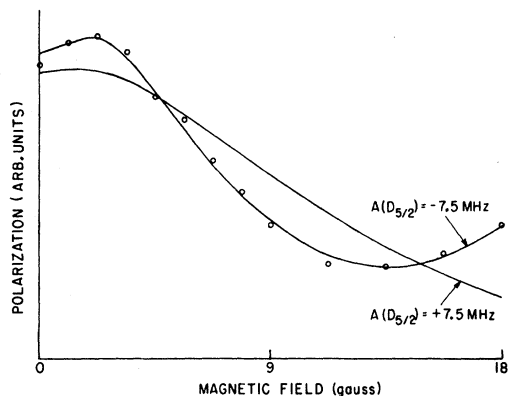


FIG. 4. Decoupling of ^{87}Rb $5D_{5/2}$ state with exciting light linearly polarized in the direction of magnetic field.

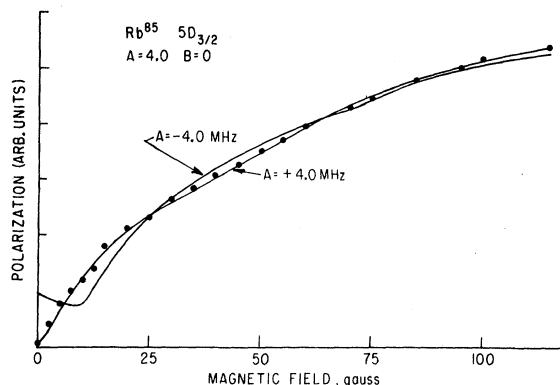


FIG. 5. Cascade-decoupling data for the $5D_{3/2}$ state of ^{85}Rb with circularly polarized light. The points are experimental data. The solid lines are calculated from the hyperfine-structure parameters indicated in the figure. These data determine the sign and the approximate magnitude of the D -state A value.

and small positive or negative values of B .

Some typical decoupling data are shown in Figs. 3–8. The decoupling data are not too sensitive to the magnitudes of A , which are determined, for the most part, by rf spectroscopy (see Sec. III C). Also, the decoupling method is not too sensitive to the lifetimes of the excited states, but decoupling data do clearly determine the signs of the coupling constants A . The decoupling curves in Fig. 3 were taken with circularly polarized exciting and detected light, and they show very clearly that the sign of A is positive for the $5^2D_{3/2}$ state of Rb^{87} but negative for the $5^2D_{5/2}$ state. Similar decoupling data for linearly polarized light are shown in Fig. 4, and again it is clear that the sign of A is negative for the $5^2D_{5/2}$ state of ^{87}Rb . In this case a magnitude $|A| = 7.5$ MHz fits the data slightly better than 8.0 MHz, which gave the best fit to the data of Fig. 3. The uncertainty in the actual magnitude of the coupling constants as deduced from theoretical fits to the decoupling curves is probably largely owing to uncertainties in our knowledge of the spectral profile of the exciting light, and for this reason we have deduced the magnitudes for A from rf data if possible.

Decoupling data for the $5^2D_{5/2}$ state of ^{85}Rb are shown in Fig. 6. Again we conclude that A is negative. The data in Fig. 6 were obtained with circularly polarized light.

In the case of $6^2D_{3/2}$ state of ^{133}Cs , there is an accidental coincidence between the cesium $6^2S_{1/2} \rightarrow 8^2P_{1/2}$ transition frequency and the strong helium line at 3888.65 Å. Heavy alkali metals are known to have anomalously small oscillator strengths for ground state to $n^2P_{1/2}$ state transitions.¹¹ This anomaly increases with increasing n . Therefore

it is extremely difficult to achieve enough population of the $6^2D_{3/2}$ state by cesium-resonance-line excitation. However, the helium 3888.65-Å line is sufficiently strong that a good signal-to-noise ratio can be obtained using this method of excitation. An interesting feature of excitation by helium light is that it excites atoms to the $8^2P_{1/2}$ state mainly out of the $F=4$ hyperfine sublevel of the ground state.¹² Decoupling curves for the $6^2D_{3/2}$ state of ^{133}Cs are shown in Fig. 7. In this case the theoretical curves are calculated from the comprehensive version of Eq. (3), which takes the spectral profile of the exciting light into account according to Eq. (6). It is absolutely essential to take the spectral profile of the exciting light into account in this case since the excitation by 3888 Å helium light is not even approximately "white." A more detailed description of the theory of cascade-decoupling experiment for nonwhite excitation is contained in the dissertation of Tai.¹³

Decoupling data for the $6^2D_{5/2}$ state of ^{133}Cs are shown in Fig. 8. Here natural resonance light from a cesium lamp was used to excite the atoms, and the spectral profile was sufficiently "white" to allow us to use Eq. (3) along with Eqs. (4) and (5) to fit the data. We should point out that the A value of the $6^2D_{5/2}$ state of cesium is obtained from the decoupling experiment alone. This is because the wavelength of the fluorescent light, 9173 Å, is too long to give a good quantum efficiency for our photomultiplier tube. Consequently, the signal-to-noise ratios are poor and the rf resonance experiment is extremely difficult. The decoupling experiment is relatively easy because the polarization of the fluorescent light nearly doubles when the field increases from 0 to 80 G, while the rf

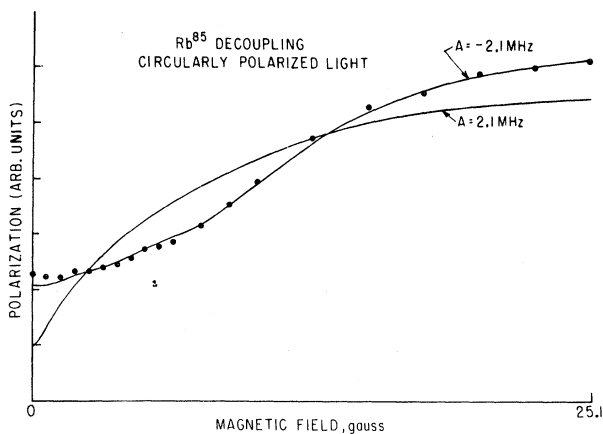


FIG. 6. Cascade-decoupling data for the $5D_{5/2}$ state of ^{85}Rb . The points are experimental data. The solid lines are calculated using the value of A indicated in the figure. These data determine the sign and the approximate magnitude of the D -state A value.

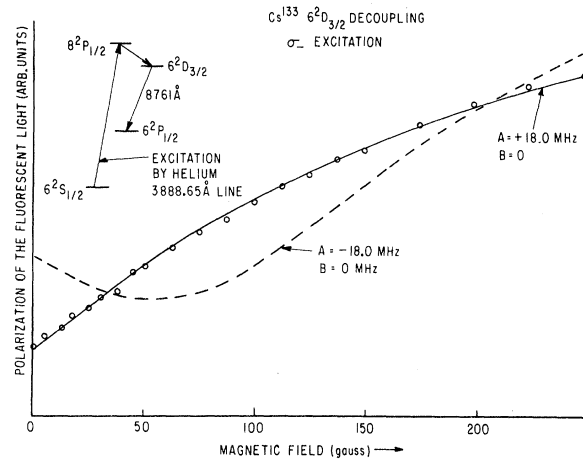


FIG. 7. Cascade-decoupling data for the $6D_{3/2}$ state of ^{133}Cs excited with circularly polarized light from a helium lamp. The lines are calculated from the hyperfine-structure parameters as shown, and the lifetime equal to 65 nsec.

resonance signal is only about 5% of the polarized fluorescence. Besides, unlike the rf resonance experiment, the thickness of the alkali-metal cell is not limited by the danger of an rf discharge. Thus we can use a thick cell to get a large signal.

B. Level crossing

Level-crossing effects can be observed in cascade experiments, as well as in more conventional experiments where cascading steps do not intervene. From (3) we see that when the levels m and n of the excited state cross, ω_{mn} passes through zero and there will be a resonant increase in the terms involving m and n in (3). However, from

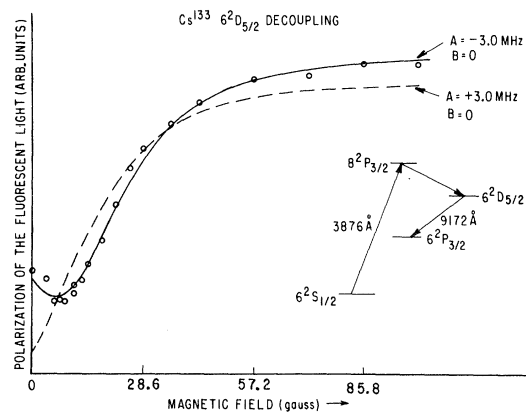


FIG. 8. Cascade-decoupling data for the $6D_{5/2}$ state excited with circularly polarized light from a Cs lamp. The lines are calculated from the hyperfine-structure parameters as shown, and the lifetime equal to 65 nsec.

the selection rules for electric dipole transitions, we see that if $M(i)$ denotes the total azimuthal quantum number of the state i , then the terms labeled by m , n , j , and k in (3) will be identically zero unless

$$M(m) - M(n) = M(j) - M(k). \quad (11)$$

The azimuthal quantum numbers of the states m and n cannot be the same if the energies $E(m)$ and $E(n)$ cross. Consequently, we conclude that $j \neq k$ for those values of j and k which contribute to a level crossing signal between the states m and n .

At high magnetic fields where the frequency differences ω_{mn} and ω_{jk} in (3) are much bigger than Γ_e and Γ_b , respectively, the "off-diagonal" terms with $m \neq n$ or $j \neq k$ will normally be much smaller than the diagonal terms with $m = n$ or $j = k$ because of the large energy denominators in the off-diagonal case. In general, when $\omega_{mn} = 0$ for a pair of excited state sublevels m and n , there will be no branch-state sublevels for which $\omega_{jk} = 0$ and vice versa. Consequently, although level crossings in the excited or branch states will lead to a resonant change in (3), the magnitude of the change will be so small compared to the diagonal terms that it will be hard to detect. The one exception to this type of behavior is at zero magnetic field where many sublevels of both the excited and branch states cross simultaneously. Thus we expect to see excellent zero-field-level crossing signals (i.e., Hanle-effect¹⁴ signals) but very small high-field crossing signals.

Nevertheless, we have succeeded in observing a high-field level-crossing signal in the $6^2D_{3/2}$ state of ^{133}Cs . Some typical data are shown in Fig. 9. The low-field Hanle-effect signal is large and symmetric, while the high-field level-crossing signals are very small and antisymmetric. The change in symmetry is brought about by the additional factor of i in (3) for the out-of-resonance

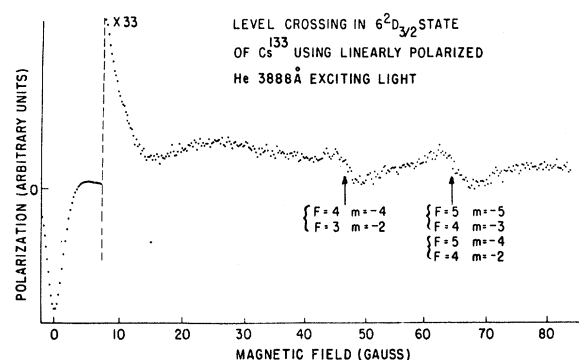


FIG. 9. Level-crossing signals in the $6^2D_{3/2}$ state of ^{133}Cs . The signal near 65 G is due to two unresolved level crossings.

denominator for a high-field level crossing.

We were able to succeed in performing a high-field cascade-level-crossing experiment in the $6^2D_{3/2}$ state of ^{133}Cs because of a lucky accident of nature. The very bright 3888-Å line of helium very nearly coincides with the third resonance line of cesium. Our experimental arrangement was essentially the same as that of the cascade-decoupling experiment, except that there is no quarter-wave plate used in the level-crossing experiment. The helium lamp we used is a quartz cell 1 cm in diameter and about 2.5 cm long, with about 4–5 Torr of helium. It is placed inside a microwave cavity, and a commercial diathermy unit is used as the source of microwave power. The exciting light is linearly polarized in a direction perpendicular to the magnetic field. A rotating HN-7 linear polarizer is used to modulate the fluorescent beam. The same lock-in amplifier is used to read the ac signal. The output of the lock-in amplifier is sent to the PDP8/S computer and a sweeping coil is used to sweep the magnetic field. Since the level-crossing signal is extremely small (about 4×10^{-4} of dc signal), we integrated for about 20 h for each of several 15-G intervals to get the composite level-crossing curve. The level-crossing experiment gives $A = 16.5 \pm 0.5$ MHz, in good agreement with the value obtained from the rf resonance experiment.

This is the first successful cascade-level-crossing experiment at high fields that we know of. Although it is not a very promising technique, in general, because of the poor signal-to-noise ratio, it is interesting to see that the phenomenon does exist, as predicted by (3). In this special case the signal yields a value of A for the $6^2D_{3/2}$ state of cesium which is about as precise as the value from rf spectroscopy (see Sec. C).

C. Radio-frequency spectroscopy

The apparatus for the rf spectroscopy is essentially the same as for the decoupling experiment shown schematically in Fig. 2, except for the replacement of the alkali cell and oven with a new cell and an rf half-wave resonator, the addition of a rf power supply, and the signal averager.

As shown in Fig. 10 the resonance box used for our experiment is a copper half-wave resonance box designed for 404 MHz. It is tunable from 400 to 415 MHz through a capacitor. Since the resonance frequency is determined mainly by the length of the central bar, further adjustment can be achieved by changing the size of the bar. It is designed in this way so that the resonance cell sits at the position of a maximum rf magnetic field and a minimum rf electric field to prevent dis-

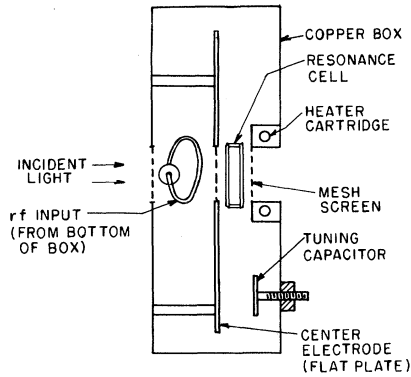


FIG. 10. Schematic diagram of the rf resonance box.

charging.⁷ A "Bird" model 7000 "High-power rf source" is used to feed the box through a coupling loop. With this box and a thin cell, we can easily feed 70 W of rf power at a cell temperature of 120°C without causing a discharge. Two cartridge heaters are used to heat the cell.

Since the fluorescent polarization at the rf resonance changes by only a fraction of the total polarization (typically about 5%), we have to integrate the signal for a long time to get a good signal-to-noise ratio. This signal averaging is achieved with a PDP8/S computer.

A signal-averaging program is used to make the computer sweep the longitudinal magnetic field repetitively. At each step, it adds the output of the lock-in amplifier, which is proportional to the intensity of polarized fluorescence, to the previous total for that field. The sweeping magnetic field, which provides a change of up to 60 G, is produced by a second pair of Helmholtz coils. The field of the main coils is kept fixed, near the expected resonance field.

The operating temperature is the same as that

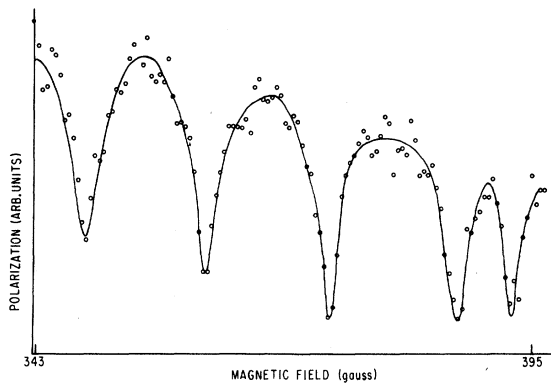


FIG. 11. Observed rf resonances in $^{87}\text{Rb } 5D_{3/2}$ state with ^{87}Rb lamp. The resonance at highest field is a $8P_{1/2}$ resonance. Radiofrequency is 403 MHz.

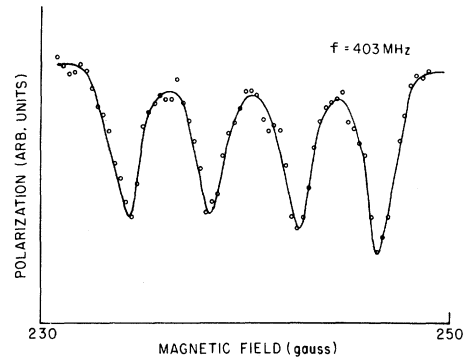


FIG. 12. rf resonances in $^{87}\text{Rb } 5D_{5/2}$ state.

in the decoupling experiment. Since decoupling experiments give us a fairly accurate value for the hyperfine interval, we can locate the excited-state resonances without undue difficulty. Generally, at first we cover a large range of magnetic field by changing the sweeping-field range. Thus we are able to see all the P - and D -state resonances, and we can be sure that they are true signals with the correct width, number of resonances, and relative position. Then we take more extensive data for the D resonances to obtain good signal-to-noise ratios. The P resonances can be used to check the calibration of the magnetic field. The hyperfine constant is calculated from the separation of these D -state resonances, in accordance with Eq. (10).

Some typical rf resonances are shown in Figs. 11–16. In all of these data circularly polarized exciting and detected light were used. In the data

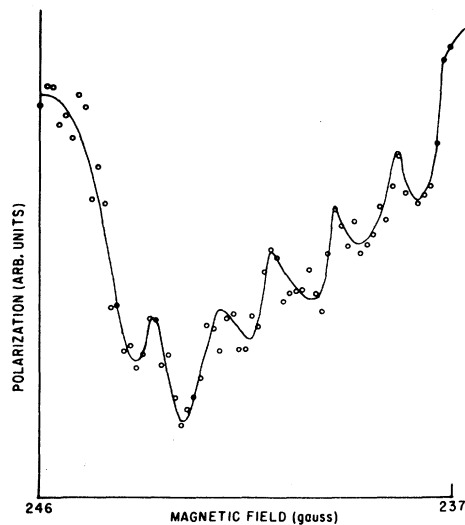


FIG. 13. rf resonances in $^{85}\text{Rb } 5D_{5/2}$ state. Radiofrequency is 403 MHz.

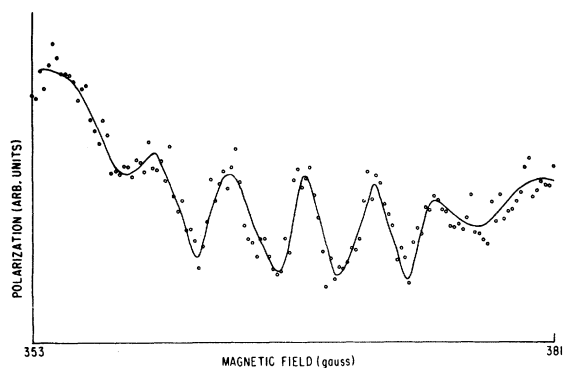


FIG. 14. Observed rf resonances in $^{85}\text{Rb } 5D_{3/2}$ state. Radiofrequency is 403 MHz.

of Figs. 15 and 16 we deliberately used nonwhite exciting light and we scanned a large enough range of magnetic field to sample magnetic resonance transitions in the 2P feeder states as well as in the D states of interest. As we shall explain in Sec. III D, one can determine the signs of the D -state A values by simple inspection of the data in Figs. 15 and 16.

D. Determination of the sign of A by narrow-line optical excitation and radiofrequency spectroscopy

Although the sign of A can be determined from decoupling experiments, it is useful to have an independent determination of the sign. In the case of the $6^2D_{3/2}$ state of cesium we may determine the sign of A by making use of the nonwhite character of the optical excitation by the 3888-Å line of helium. As we have indicated in Fig. 17, the 3888-Å line of helium excites mainly out of the

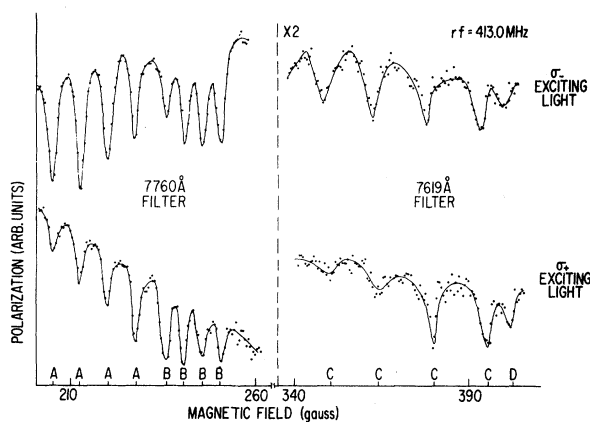


FIG. 15. rf resonances in $^{87}\text{Rb-}5D$ states with ^{85}Rb lamp. $A, B, C,$ and D refer to rf resonances in the $7P_{3/2}, 5D_{5/2}, 5D_{3/2},$ and $7P_{1/2}$ states, respectively.

$F=4$ hyperfine sublevel of the $6^2S_{1/2}$ ground state of cesium, because the helium line does not overlap the cesium absorption line perfectly. We operate at a field at which F and m_F are still quite good quantum numbers for the ground state while m_I and m_J are fairly good quantum numbers for the excited state. Such a regime is possible because the ground-state hyperfine structure is much larger than the excited-state hyperfine structure. Under these conditions σ_+ light, as indicated in Fig. 17, will excite only those excited-state sublevels with $m_J = +\frac{1}{2}$. Furthermore, the states with different values of m_I will be excited at different rates, and one can use the selection rules for electric dipole transitions to show that the populations $n(m_I, m_J)$ of sublevels with quantum numbers m_I and m_J will be

$$n(m_I, m_J) = C \times (I - m_I + 1) \quad (12)$$

where C is a constant of proportionality.

If rf transitions are induced between the sublevels, the resonance signals corresponding to sublevels with different m_I will have different amplitude. If we sweep the rf frequency while keeping the magnetic field fixed, we will get a resonance pattern as shown in Fig. 17. The relative amplitude will identify the resonances. In the case of cascade excitation, since the nuclear polarization is not changed at all by spontaneous decay at high field, the nuclear polarization will be the same throughout the cascade process. In Fig. 17, we have considered a $S_{1/2}$ branch state rather than a $D_{3/2}$ or $D_{5/2}$ state for the sake of simplicity. In this example, the $7S_{1/2}$ state will

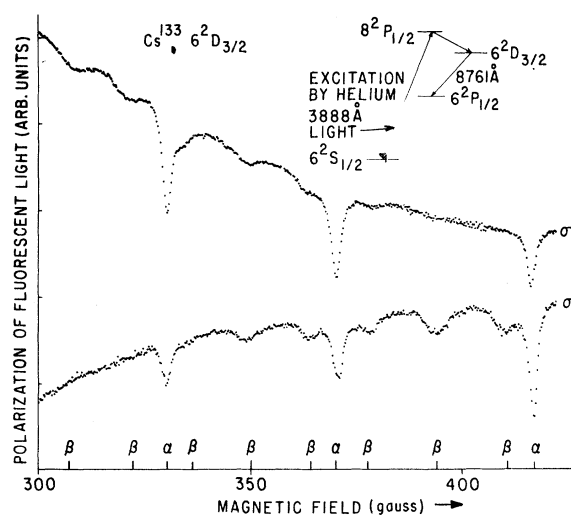


FIG. 16. rf resonances in ^{133}Cs . The symbols α and β refer to rf resonances in the $8P_{1/2}$ and $6D_{3/2}$ states, respectively. Cs atoms were excited by helium 3888-Å light in this case.

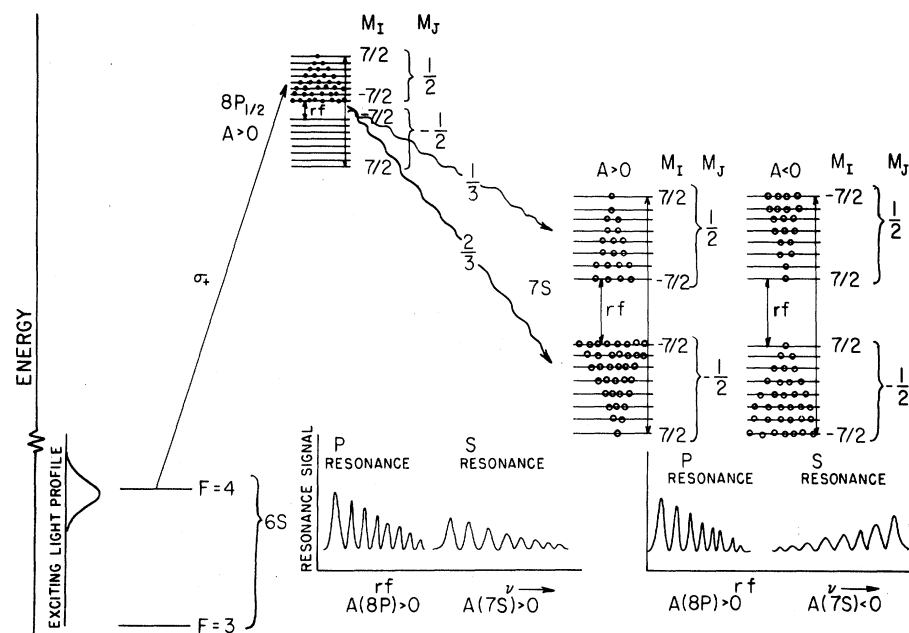


FIG. 17. Cascade rf spectroscopy of ^{133}Cs with "nonwhite" excitation. Cs vapor is excited with circularly polarized light from a helium lamp. The magnetic field is about 700 G in the example shown here. The relative amplitudes of the resonance signals can be used to determine signs of magnetic dipole coupling constants A for the excited and the branch states.

have the same nuclear polarization as the $8P_{1/2}$ state and the resonance signals induced between the hyperfine sublevels will still have amplitudes proportional to $I - m_I + 1$. In the example sketched in Fig. 17, one would observe a series of eight resonances ($2I + 1 = 8$ for ^{133}Cs) with amplitudes which decrease in order of increasing magnetic resonance frequency if the sign of A is positive for the $7S$ state. However, if the sign of A were negative for the $7S$ state the amplitudes of the rf resonances would increase in order of increasing magnetic resonance frequency, because now the states with the largest population differences (those with $m_I < 0$) are also further apart at a given magnetic field. It is not even necessary to know whether the exciting light has σ_+ or σ_- polarization, since this is determined by the trend of the resonance amplitudes for the $8P_{1/2}$ state. The low-frequency resonances are stronger for σ_+ excitation, the high-frequency resonances are stronger for σ_- excitation. By comparing the trends of the observed resonances for the excited state (the $8P_{1/2}$ state) and the branch state (the $7S_{1/2}$ state) which it feeds it is possible to determine the relative signs of A for the two states. If the trends are the same, the A values for the two states have the same signs; if the trends are opposite the A values have opposite signs.

For electrons cascading to the $6D_{3/2}$ state, although the distribution of the population of electrons among different m_J sublevels is more complicated, the distribution among different m_I sublevels is still proportional to $I - m_I + 1$. This re-

lation holds for further cascade and is very useful in the determination of the sign of the hyperfine constant A .

To further illustrate this point, ^{87}Rb vapor was excited by resonance light from a ^{85}Rb lamp. Since the hfs of the ground state of ^{87}Rb is 6.8 GHz while for ^{85}Rb it is only 3.3 GHz, the ^{87}Rb atoms are excited mainly out of $F=2$ hyperfine sublevel of the ground state. The rf results are shown in Fig. 15. An inspection of the data of Fig. 15 shows that A is negative for the $5D_{5/2}$ state of ^{87}Rb , and positive for the $5D_{3/2}$ state, in agreement with the conclusion drawn in Sec. III A from the decoupling data. Similarly, we see from inspection of the data of Fig. 16 that A is positive for the $6D_{3/2}$ state of ^{133}Cs .

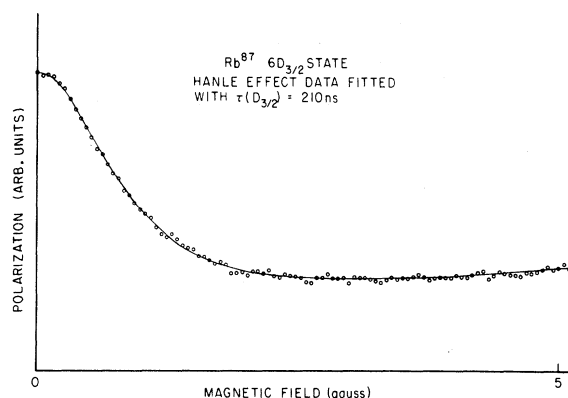


FIG. 18. Hanle-effect data for the $5D_{3/2}$ state of ^{87}Rb . The solid line is the least-squares-fitted curve.

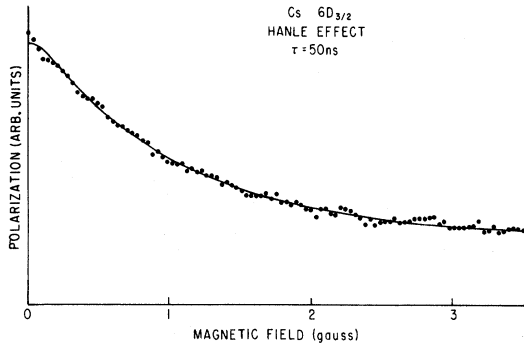


FIG. 19. Least-squares-fitted Hanle-effect curve for the $6\ ^2D_{3/2}$ state of ^{133}Cs .

E. Cascade Hanle effect

In order to measure the lifetimes of the D states, cascade-Hanle-effect experiments were performed with essentially the same apparatus as that used to measure decoupling curves. The only difference was that both the exciting and detected light were polarized in such a way as to couple to the transverse atomic coherence. The cascade Hanle effect is also described by Eq. (3) and we deduced D -state lifetimes by using computer-generated solutions of (3) to fit our data, as described in Sec. IIIA. Of course the lifetime of the feeding P states must be known to analyze the Hanle-effect data, and the curves also depend somewhat on the hyperfine structures of the excited and branch states. The Hanle-effect signals also depend very strongly on the spectral profile of the exciting light. Although we tried to account for all of these factors, the uncertainties were such that our lifetime measurements are not very precise. Typical data and fits are shown in Figs. 18 and 19. The fitted values of lifetimes in Figs. 18 and 19 are slightly different from the values shown in Table II (see

Sec. IV). This is because the final values listed in Table II are the best values deduced from many repeated runs of the type shown in Figs. 18 and 19.

IV. RESULTS AND DISCUSSION

A. Results

A compilation of the experimental results of the A value is shown in Table I. The rf resonance results were obtained from several repeated measurements, and the quoted error bars represent three standard deviations in the statistical spread of the results plus an allowance for any systematic errors, such as errors in the magnetic field calibration, etc. Table I also shows some upper limits on the electric quadrupole coupling constants B . These upper limits have been obtained by an inspection of the widths of the rf resonances shown in Figs. 11–16. As we pointed out in Sec. II in connection with Eq. (9), the B values are so small for all the states we have investigated that we do not observe resolved transitions corresponding to different values of m_j . Therefore, an accurate determination of B values is not possible in our experiments. It should be possible to obtain better estimates of the B values than those given in Table I by a careful analysis of the resonance linewidths, and the values given in Table I should only be regarded as gross upper limits. The true values may be substantially smaller. The lifetimes of D states measured in this work are given in Table II. In Table III we have listed the P state hyperfine structure and lifetimes that we have used to calculate theoretical curves from Eq. (3).

B. Comparison with theory

A simple one-particle theoretical estimate of the A value can be obtained from the following

TABLE I. Hyperfine coupling constants A and B measured in this work. The methods used are (i) rf resonance and decoupling, (ii) level crossing and decoupling, and (iii) decoupling. A is the magnetic dipole coupling constant and B is the electric quadrupole coupling constant.

Element	State	Method	Measured A (MHz)	Calculated A (MHz)	Measured B (MHz)
^{87}Rb	$5\ ^2D_{3/2}$	(i)	14.43 ± 0.23	13.57	< 3.5
	$5\ ^2D_{5/2}$	(i)	-7.44 ± 0.10	5.81	< 5
^{85}Rb	$5\ ^2D_{3/2}$	(i)	4.18 ± 0.20	4.00	< 5
	$5\ ^2D_{5/2}$	(i)	-2.12 ± 0.20	1.71	...
^{133}Cs	$6\ ^2D_{3/2}$	(ii)	16.5 ± 0.5	9.4	...
	$6\ ^2D_{3/2}$	(i)	16.30 ± 0.15	9.4	< 8
	$6\ ^2D_{5/2}$	(iii)	-3.6 ± 1.0	4.0	...

TABLE II. Radiative lifetimes measured in this work.

Element	State	Calculated ^a τ (nsec)	Measured τ (nsec)
⁸⁷ Rb	5D _{3/2}	241	205 ± 40
¹³³ Cs	6D _{3/2}	64.5	57 ± 15

^aO. S. Heavens, J. Opt. Soc. Am. 51, 1058 (1961).

equation¹⁵:

$$A_j = \frac{2\mu_B^2}{\hbar} g_I'^2 \frac{l(l+1)}{j(j+1)} F_{r,j} (1-\delta)(1-\epsilon) \langle r^{-3} \rangle, \quad (13)$$

where $g_I' = \mu_I/\mu_B I$ (nuclear g factor), l is the orbital angular momentum quantum number, δ and ϵ are corrections for the spatial extent of the charge and the magnetic dipole distribution of the nucleus, $F_{r,j}$ is a relativistic correction of the order of 1, and $\langle r^{-3} \rangle$ is the expectation value of r^{-3} , where r is the distance between the nucleus and the valence electron.

In order to estimate the hfs constant A , it is necessary to know $\langle r^{-3} \rangle$. However, the calculation of the wave function of the valence electron is difficult and does not yield very reliable values of $\langle r^{-3} \rangle$. Therefore, the fine-structure splitting, which also depends on $\langle r^{-3} \rangle$, is normally used to find $\langle r^{-3} \rangle$. In our case, however, the fine structure is anomalous. Thus, to calculate A_j we estimate $\langle r^{-3} \rangle$ by the Landé formula¹⁵

$$\langle r^{-3} \rangle = \frac{z z'^2}{n^*{}^3 l(l+1)(l+\frac{1}{2}) r_B^3}, \quad (14)$$

where n^* is the effective quantum number, z' is the effective charge that the electron sees, and r_B is the Bohr radius.

Our calculated values are given in Table I together with the measured values. We can see from this table that there is a big disagreement. Moreover, from Eq. (13), we should have the relation

$$\frac{A_{l-1/2}}{A_{l+1/2}} = \frac{l+\frac{3}{2}}{l-\frac{1}{2}}$$

apart from the relativistic correction of order 1. With $l=2$, $A_{3/2}/A_{5/2} = \frac{7}{3} = 2.33$, while our measured values give $A_{3/2}/A_{5/2} = -1.92$ and -4.5 , respect-

TABLE III. P -state parameters that were used in analyzing some of our data.

Atom	I	μ_I	State	A (MHz)	B (MHz)	Lifetime (nsec)
⁸⁵ Rb	$\frac{5}{2}$	1.3527	$7^2P_{1/2}$	17.65(2) ^a		255 ^b
			$7^2P_{3/2}$	3.71(1) ^c	3.68(10) ^c	240 ± 20 ^c
⁸⁷ Rb	$\frac{3}{2}$	2.7506	$7^2P_{1/2}$	59.92(9) ^a		255 ^b
			$7^2P_{3/2}$	12.57(1) ^c	1.768(8) ^d	233(10) ^d
¹³³ Cs	$\frac{7}{2}$	2.579	$8^2P_{1/2}$	42.97(10) ^e		330 ± 30 ^f
			$8^2P_{3/2}$	7.626(5) ^g	-0.049(42) ^g	310(15) ^h

^aD. Feiertag and G. zu Putlitz, Z. Phys. 208, 447 (1968).

^bO. S. Heavens, J. Opt. Soc. Am. 51, 1058 (1961).

^cH. Bucka, G. zu Putlitz, and R. Rabold, Z. Phys. 213, 101 (1968).

^dG. Belin and S. Svanberg, Phys. Scr. 4, 269 (1971).

^eC. Tai, R. Gupta, and W. Happer, Phys. Rev. A 8, 1661 (1973).

^fE. L. Altman, Opt. Spektrosk. 28, 1029 (1970) [Opt. Spectrosc. 28, 556 (1970)].

^gH. Bucka and C. von Oppen, Ann. Phys. 10, 119 (1962).

^hS. Svanberg and S. Rydberg, Z. Phys. 227, 216 (1969).

ively, for rubidium and cesium. We see that for the states investigated in this work there is a gross disagreement between the measurements and the predictions of a single-particle model of the alkali atom's hyperfine structure.

Liao *et al.*¹⁶ have recently measured the constants of the complete magnetic dipole hyperfine Hamiltonian of the $4D$ state of rubidium, and they have shown that in this state most of the interaction originates from a term proportional to $\vec{S} \cdot \vec{I}$ and that the effective values of $\langle r^{-3} \rangle$ for the orbital and spin-dipole parts of the hfs Hamiltonian are not the same. In fact, $\langle r^{-3} \rangle$ was found to be negative for the spin-dipole interaction. Unfortunately, in our work we obtained only two measured quantities ($A_{3/2}$ and $A_{5/2}$), while three independent measurements would be necessary to evaluate the three independent constants of the magnetic dipole hfs Hamiltonian. It would be very interesting if high-field measurements could be carried out on some of these states to provide the missing information.

*Work supported by the Joint Services Electronics Program (U. S. Army, U. S. Navy, and U. S. Air Force) under Contract No. DAAB07-74-C-0341.

†Present address: Department of Physics, University of British Columbia, Vancouver, Canada.

¹C. E. Moore, *Atomic Energy Levels*, NBS Circular No. 467 (U. S. GPO, Washington, D. C., 1949, 1952, 1958).

²Y. Archambault, J. P. Descoubes, M. Priou, A. Omont, and J. C. Pebay-Peyroula, J. Phys. Radium 21, 677 (1960).

³P. Brix and H. Kopfermann, *Festschrift Gottinger Akad.* (Springer Verlag, Berlin, 1951), p. 17; H. Kopferman, *Nuclear Moments* (Academic, New York, 1958).

⁴S. Chang, R. Gupta, and W. Happer, Phys. Rev. Lett.

- 27, 1036 (1971).
- ⁵R. Gupta, S. Chang, and W. Happer, *Phys. Rev. A* 6, 529 (1972).
- ⁶R. Gupta, S. Chang, C. Tai, and W. Happer, *Phys. Rev. Lett.* 29, 695 (1972).
- ⁷R. Gupta, W. Happer, L. K. Lam, and S. Svanberg, *Phys. Rev. A* 8, 2792 (1973).
- ⁸B. D. Fried and S. D. Conte, *The Plasma Dispersion Function* (Academic, New York, 1961).
- ⁹W. Happer, in *Beam Foil Spectroscopy*, edited by S. Bashkin (Gordon and Breach, New York, 1968).
- ¹⁰F. D. Colgrove, P. A. Franken, R. R. Lewis, and R. H. Sands, *Phys. Rev. Lett.* 3, 420 (1959); P. A. Franken, *Phys. Rev.* 121, 508 (1961).
- ¹¹G. zu Putlitz, *Comments. At. Mol. Phys.* 1, 51 (1969).
- ¹²P. Rabinowitz and S. Jacobs, in *Quantum Electronics, Proceedings of the Third International Congress*, edited by P. Grivet and N. Bloembergen (Columbia U. P., New York, 1964).
- ¹³C. Tai, dissertation (Columbia University, 1974) (unpublished).
- ¹⁴W. Hanle, *Z. Phys.* 30, 93 (1924).
- ¹⁵H. Kopfermann, *Nuclear Moments* (Academic, New York, 1958).
- ¹⁶K. H. Liao, L. K. Lam, R. Gupta, and W. Happer, *Phys. Rev. Lett.* 32, 1340 (1974).